Plant Disease • 2020 • 104:2054-2059 • https://doi.org/10.1094/PDIS-11-19-2493-SC

Short Communication

An Emerging Strawberry Fungal Disease Associated with Root Rot, Crown Rot and Leaf Spot Caused by *Neopestalotiopsis rosae* in Mexico

Angel Rebollar-Alviter,[1,†] Hilda Victoria Silva-Rojas,[2] Dionicio Fuentes-Aragón,[3] Uriel Acosta-González,[1] Merari Martínez-Ruiz,[4] and Brenda Estefanía Parra-Robles[5]

[1] Universidad Autónoma Chapingo, Centro Regional Morelia, Morelia, Michoacán, México
[2] Producción de Semillas, Colegio de Postgraduados, Campus Montecillo, Texcoco, Estado de México, México
[3] Posgrado en Fitosanidad, Colegio de Postgraduados, Campus Montecillo, Texcoco, Estado de México, México
[4] Posgrado en Protección Vegetal. Universidad Autónoma Chapingo, Texcoco, Estado de México, México
[5] Departamento de Parasitología Agrícola, Universidad Autónoma Chapingo, Texcoco, Estado de México, México

Abstract

In the 2017 strawberry season, several transplant losses reaching 50% were observed in Zamora, Michoacán Valley, Mexico, due to a new fungal disease associated with root rot, crown rot, and leaf spot. In this year the disease appeared consistently and increased in the following seasons, becoming a concern among strawberry growers. Thus, the aim of this research was to determine the etiology of the disease and to determine the in vitro effect of fungicides on mycelial growth of the pathogen. Fungal isolates were obtained from symptomatic strawberry plants of the cultivars 'Albion' and 'Festival' and were processed to obtain monoconidial isolates. Detailed morphological analysis was conducted. Concatenated phylogenetic reconstruction was conducted by amplifying and sequencing the translation elongation factor 1 α, β-tubulin partial gene, and the internal transcribed spacer region of rDNA. Pathogenicity tests involving inoculation of leaves and crowns reproduced the same symptoms as those observed in the field, fulfilling Koch's postulates. Morphology and phylogenetic reconstruction indicated that the causal agent of the described symptoms was *Neopestalotiopsis rosae*, marking the first report anywhere in the world of this species infecting strawberry. *N. rosae* was sensitive to cyprodinil + fludioxonil, captan, iprodione, difenoconazole, and prochloraz.

Keywords: crown rot, *Neopestalotiopsis* sp., strawberry, etiology

During the strawberry (*Fragaria* × *ananassa* Duch.) production season, between February and April 2017, severe wilting symptoms that began with slight yellowing of the outer leaves, progressing toward the central leaves until the plants collapsed, were observed on the cultivars 'Albion' and 'Festival'. Close inspection of the split crowns showed irregular areas of a reddish color, sometimes with dark brown edges, which began at the margin of the crown (Fig. 1).

In the 2018 to 2019 production season, from August to November, leaves of strawberry transplants of the same varieties showed small spots, dark brown in color, of approximately 1 mm, which progressed concentrically. These leaf spots spread to more extensive areas, resulting in severe leaf blight. On petioles, sunken dark brown lesions were also observed, which progressed toward the base of the petiole, reaching the crown and causing leaf wilting. Roots of symptomatic plants were dark brown in color. The crowns showed irregular reddened areas with dark brown edges, similar to the features described in the previous season. Overall, the diseased plants showed reduced growth and died approximately 1 month after transplanting. The symptoms described were observed with higher intensity in strawberry plantations established in open fields and exposed to rain than in those plantations established in high tunnels with temperatures between 23 and 27°C. In this production system, it was observed that most of the transplant losses occurred in crop beds that were exposed to rain, suggesting that the disease is associated with the presence of rain and long periods of leaf wetness and that the causal agent(s) may be splash-dispersed. In the crop cycle of 2019 to 2020, the disease was again observed from the beginning of July 2019 in newly established transplants, showing the previously described symptoms under the same weather conditions in the cultivars 'Festival', 'Fortuna', 'Frontera', 'Rociera', 'Cabrillo', and 'Albion.' In the last 2 seasons, strawberry producers indicated that the losses were estimated at between 40 and 50% of established transplants, but there is no information regarding the source of the primary infections. In Mexico, strawberry production is based on plants imported from other countries, such as the United States, Chile, and Spain. Similar symptoms to those described here have been recently associated with *Pestalotiopsis* (*Neopestalotiopsis* sp.) and *Neopestalotiopsis clavispora* in Italy (Gilardi et al. 2019), Mexico (Morales-Mora et al. 2019), Spain (Chamorro et al. 2016), the United States (Mertely et al. 2019), and Uruguay (Machín et al. 2019). Therefore, the aims of this study were to determine the causal agent of strawberry leaf spot, blight, and crown rot in Mexico and to evaluate the in vitro activity of commonly used fungicides in strawberry production against this pathogen.

In September 2018, five commercial plots were sampled in the municipalities of Zamora and Jacona, Michoacán, and 10 plants were selected per plot with the symptoms previously described. Sections of 0.5 cm corresponding to the crown tissue, leaves, and symptomatic petioles were disinfested with 2% sodium hypochlorite for 2 min and rinsed three times with sterile distilled water. The tissue portions were placed in a laminar flow hood to remove excess moisture and then placed in Petri dishes with potato dextrose agar (PDA) medium (Bioxon). Finally, the plates were incubated at laboratory temperature (22 ± 2°C). Additionally, symptomatic foliar tissues, petioles, crowns, and runners were placed in a humid chamber and incubated under the same conditions to promote fungal sporulation. The colonies that grew from the different plant tissues were purified and incubated until the formation of conidia.

†Corresponding author: A. Rebollar-Alviter; rebollaralviter@gmail.com

Funding: Funding was provided by Universidad Autonoma Chapingo (grant no. 19271-C-63).

The author(s) declare no conflict of interest.

Accepted for publication 26 February 2020.

© 2020 The American Phytopathological Society

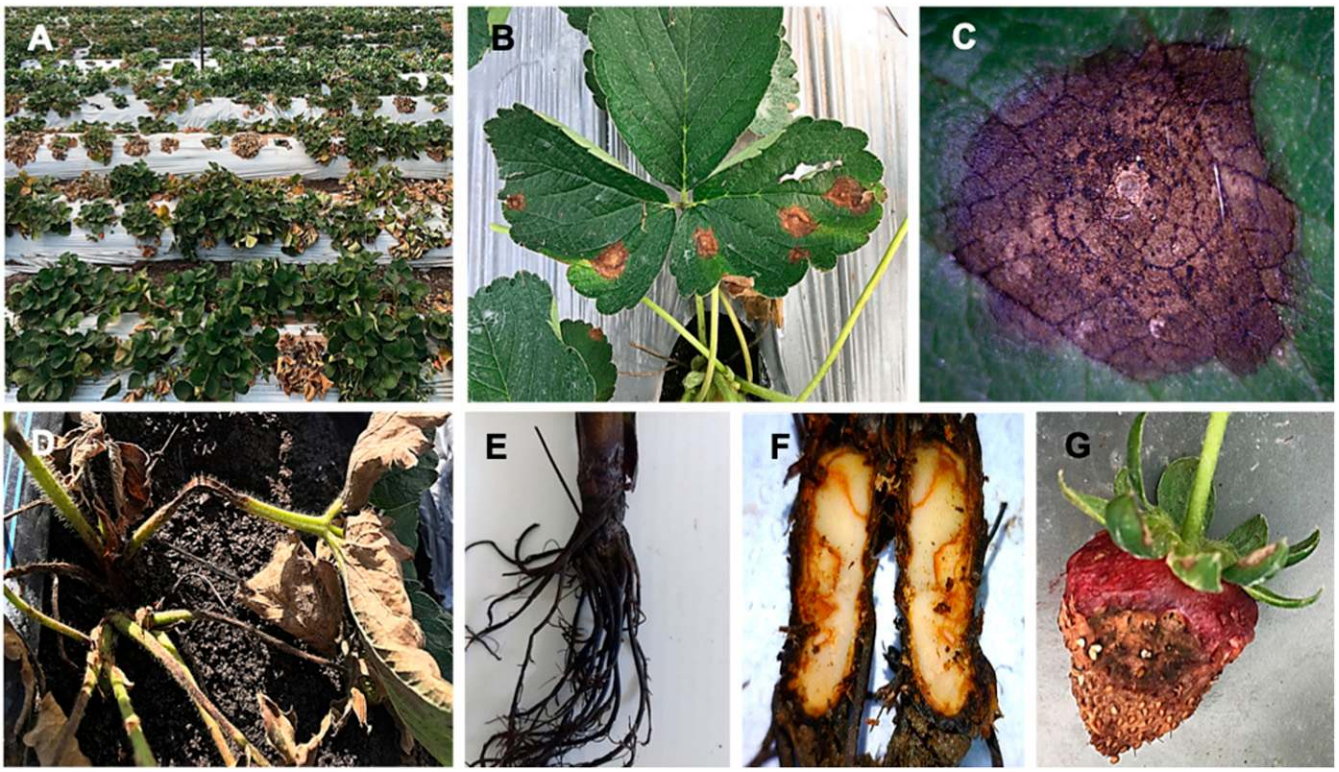

Fig. 1. Field symptoms development associated with *Neopestalotiopsis rosae*: **A,** commercial field with strawberry plants showing plant collapse associated with crown rot symptoms; **B,** typical symptoms on strawberry leaves; **C,** close-up of leaf spot showing acervuli with conidia; **D,** disease symptoms on leaf petioles; **E,** root rot; **F,** crown rot symptoms; and **G,** typical symptoms on strawberry fruits.

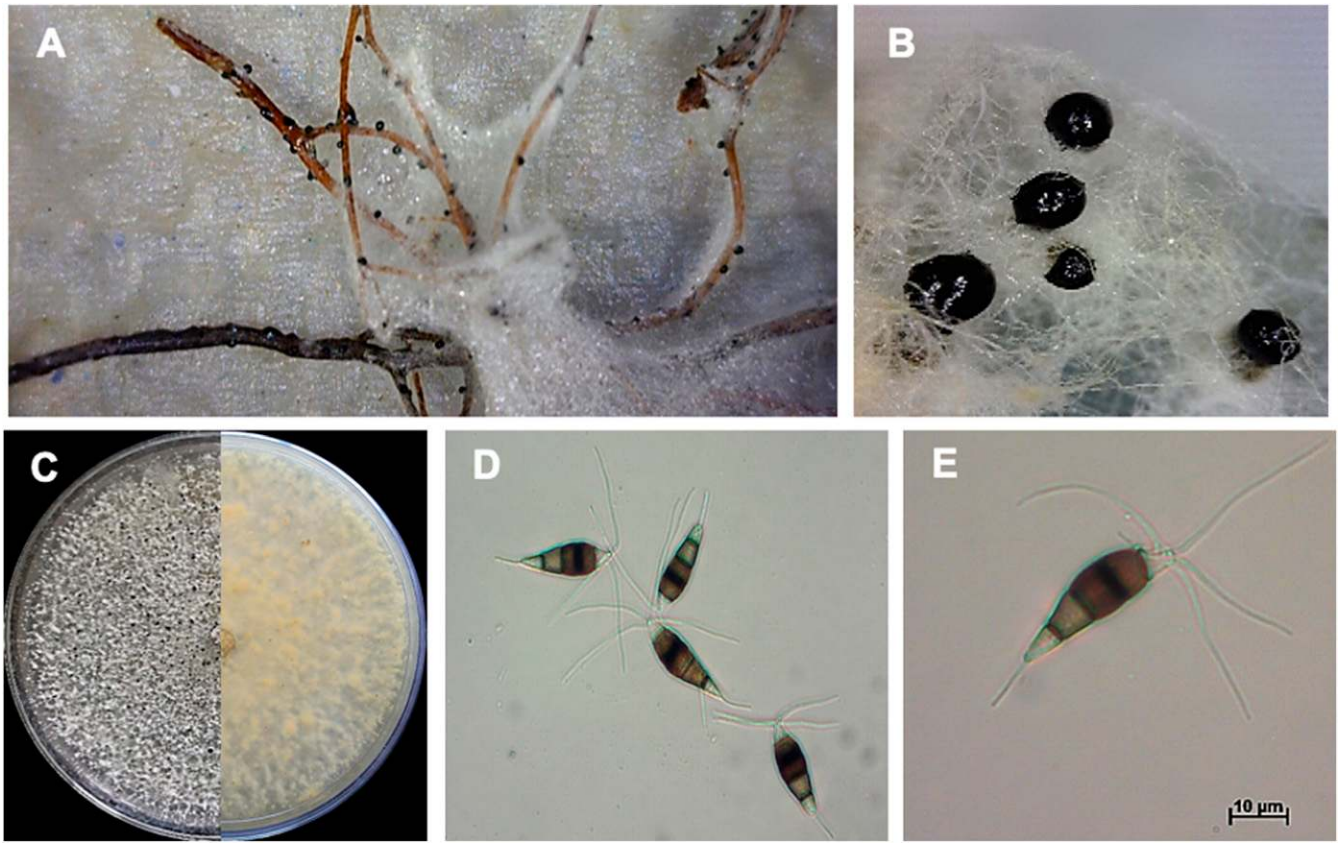

Fig. 2. *Neopestalotiopsis rosae*: **A,** acervuli on strawberry roots formed in a moist chamber; **B,** close-up of acervuli of *N. rosae*; **C,** culture characteristics; and **D** and **E,** conidia of *N. rosae* formed on PDA medium.

Neopestalotiopsis sp. was preliminarily identified from leaves, petioles, runners, roots, and crowns based on the characteristics described by Maharachchikumbura et al. (2014). From these isolates, 10 monoconidial isolates were obtained after 10 days of incubation on a laboratory bench. An isolate from leaves designated CRM-FRH and one from the strawberry crown called CRM-FRC were selected. On PDA medium, these isolates produced a cottony white mycelium with abundant dark-colored acervuli, with the presence of conidia 10 days after plating. The acervuli produced five-celled fusiform to ellipsoidal conidia, with the three central cells being dark in color and the basal cells being hyaline. Fifty conidia of each isolate were measured at 40× magnification using a Carl Zeiss microscope (Primo Star Model, Germany). The conidia of the CRM-FRH isolate measured (n = 100; length × width) 22.34 to 34.12 × 6.0 to 11.07 μm (average 27.29 × 8.33 μm), and the CRM-FRC varied from 20.6 to 33.5 × 5.32 to 8.76 μm (average 26.43 × 7.08 μm). The conidia presented mostly three and less frequently four apical appendages (Fig. 2).

DNA extraction was carried out for the CRM-FRH and CRM-FRC strains using the cetyl trimethylammonium bromide 2% protocol (Doyle and Doyle 1990) with slight modifications. Polymerase chain reaction amplifications of the translation elongation factor 1 α (*tef1*), β-tubulin (*tub2*) partial gene, and the internal transcribed spacer (ITS) region were carried out with the EF-1 + EF-2 (O'Donnell et al. 1998), T1 + Tb2t (O'Donnell and Cigelnik 1997; Glass and Donaldson 1995), and ITS5 + ITS4 (White et al. 1990) primers, respectively. Amplicons were cleaned using ExoSAP-IT (Affymetrix, U.S.A.) and sequenced in both directions at the Postgraduate College sequencing facility (Texcoco, Mexico) according to the method of Juárez-Vázquez et al. (2019).

Consensus sequences were created with BioEdit version 5.0.9 (Hall 1999). Alignments were performed using MAFFT online service (https://mafft.cbrc.jp/alignment/server/). Maximum likelihood (ML) and Bayesian inference (BI) procedures were implemented using the raxmlGUI (Silvestro and Michalak 2012) and MrBayes (Ronquist et al. 2012) software, respectively. In the first phylogenetic reconstruction using only BI, sequences belonging to the ITS region of some *Pestalotiopsis*, *Pseudopestalotiopsis*, and *Neopestalotiopsis* species were included, with the aim of assigning the strains obtained in this study to genera. In the second reconstruction, phylogenetic analysis was performed for the genus *Neopestalotiopsis*, including all strains reported on *Fragaria* worldwide. For ML procedures, a rapid bootstrapping analysis with 1,000 repetitions was carried out, and the GTR + Γ nucleotide substitution model was considered in the analysis. For BI, two parallel analyses with four Markov chain Monte Carlo algorithms were performed, the analyses were stopped until reaching a standard deviation of split frequencies (SDSF) < 0.01, and trees were sampled every 1,000 iterations. Substitution models were previously selected using jModelTest software (Darriba et al. 2012) and implemented

Table 1. Characteristics of species and strains of *Pestalotiopsis*, *Pseudopestalotiopsis*, and *Neopestalotiopsis*, including GenBank accession numbers, used for phylogenetic reconstruction. The strains and sequences obtained in this research are in bold.

Species	Strain[a]	Country	Host	GenBank accessions[b]		
				ITS	*tub2*	*tef1*
N. australis	CBS 114159*	Australia	*Telopea* sp.	KM199348	KM199432	KM199537
N. clavispora	MFLUCC 12-0281*	China	*Magnolia* sp.	JX398979	JX399014	JX399045
	TOR-802-803-804	Spain	*Fragaria* × *ananassa*	KU096879	KU096880	KU096881
N. cubana	CBS 600.96	Cuba	Leaf litter	KM199347	KM199438	KM199521
N. ellipsospora	MFLUCC 12-0282*	China	Dead plant materials	JX398980	JX399016	JX399047
	MFLUCC 12-0284	Thailand	Dead plant materials	JX398981	JX399015	JX399046
N. eucalypticola	CBS 264.37*	…	*Eucalyptus globulus*	KM199376	KM199431	KM199551
N. foedans	CGMCC 3.9123*	China	Mangrove plant	JX398987	JX399022	JX399053
	CGMCC 3.9178	China	*Neodypsis decaryi*	JX398989	JX399024	JX399055
N. formicarum	CBS 362.72*	Ghana	Dead Formicidae	KM199358	KM199455	KM199517
	CBS 115.83	Cuba	Plant debris	KM199344	KM199444	KM199519
N. honoluluana	CBS 114495*	U.S.A.	*Telopea* sp.	KM199364	KM199457	KM199548
N. iranensis	CBS 137768*	Iran	*Fragaria* × *ananassa*	KM074048	KM074057	KM074051
N. javaensis	CBS 257.31*	Indonesia	*Cocos nucifera*	KM199357	KM199437	KM199543
N. mesopotamica	CBS 336.86*	Iraq	*Pinus brutia*	KM199362	KM199441	KM199555
	CBS 299.74	Turkey	*Eucalyptus* sp.	KM199361	KM199435	KM199541
	CBS 137766	Iran	*Fragaria* × *ananassa*	KM074047	KM074058	KM074054
N. piceana	CBS 394.48*	UK	*Picea* sp.	KM199368	KM199453	KM199527
	CBS 254.32	Indonesia	*Cocos nucifera*	KM199372	KM199452	KM199529
	CBS 225.30	…	*Mangifera indica*	KM199371	KM199451	KM199535
N. rosae	CBS 101057*	New Zealand	*Rosa* sp.	KM199359	KM199429	KM199523
	CBS 124747	U.S.A.	*Paeonia suffruticosa*	KM199360	KM199430	KM199524
	CRM-FRC	**Mexico**	***Fragaria* × *ananassa***	**MN385718**	**MN268529**	**MN268532**
	CRM-FRH	**Mexico**	***Fragaria* × *ananassa***	**MN385719**	**MN268530**	**MN268533**
	CRM-FRC2	**Mexico**	***Fragaria* × *ananassa***	**MN385720**	**MN268531**	**MN268534**
N. saprophytica	CBS 115452*	China	*Litsea rotundifolia*	KM199345	KM199433	KM199538
N. steyaertii	IMI 192475*	Australia	*Eucalyptus viminalis*	KF582796	KF582794	KF582792
N. zimbabwana	CBS 111495*	Zimbabwe	*Leucospermum cuneiforme*	JX556231	KM199456	KM199545
Neopestalotiopsis sp.	CBS 323.76	France	*Erica gracilis*	KM199350	KM199458	KM199550
	CBS 266.37	Germany	*Erica* sp.	KM199349	KM199459	KM199547
	CBS 119.75	India	*Achras sapota*	KM199356	KM199439	KM199531
	CBS 266.80	India	*Vitis vinifera*	KM199352	…	KM199532
	CBS 361.61	Netherlands	*Cissus* sp.	KM199355	KM199460	KM199549
	CBS 360.61	Guinea	*Cinchona* sp.	KM199346	KM199440	KM199522
	CBS 164.42	France	Dune sand	KM199367	KM199434	KM199520
Pseudopestalotiopsis indica	CBS 459.78*	India	*Hibiscus rosa-sinensis*	KM199381	KM199470	KM199560

[a] Asterisk (*) indicates ex-holotype or ex-type culture.
[b] ITS = internal transcribed spacer; *tub2* = β-tubulin; and *tef1* = translation elongation factor 1 α.

in BI. The first 25% of trees generated were discarded as the burn-in phase, and the posterior probability (PP) was calculated with the remaining trees. The trees were visualized and edited in FigTree version 1.4.4 (http://tree.bio.ed.ac.uk/software/figtree/), and the sequences obtained in this study (Table 1) were deposited in the GenBank database (https://www.ncbi.nlm.nih.gov/genbank/).

The phylogenetic analysis of the ITS region consisted of 45 sequences and 573 characters, including gaps. *Sordaria tomento-alba* CBS 260.70 was used as the outgroup. In this analysis, 1,000,000 iterations were run with the Hasegawa–Kishono–Yano model implemented, generating 1,002 trees, of which 752 were used to calculate the PPs. The phylogeny of the ITS region precisely delimited the three genera proposed by Maharachchikumbura et al. (2014). The strains obtained in this study were grouped with the clade *Neopestalotiopsis*; however, it was not possible to distinguish between the species *N. rosae*, *N. clavispora*, *N. javaensis*, and *Neopestalotiopsis* sp. (Fig. 3). In addition, *Pestalotiopsis* sp. (MK713562), reported in Mexico causing leaf spot and strawberry anthracnose (Morales-Mora et al. 2019), grouped in the clade of *Neopestalotiopsis*. *N. clavispora* has been reported in several countries in association with crown rot symptoms. However, most isolates were identified by BLAST analysis of the ITS region (Gilardi et al. 2019; Obregón et al. 2018), which cannot delimit various species of *Neopestalotiopsis*. The multilocus analysis (*tef1*, *tub2*, ITS) consisted of 36 sequences and 2,002 characters; 600,000 iterations were run (SDSF = 0.008904), with the GTR + G model for *tub2* and *tef1*, and GTR + I model for the ITS, generating 1,202 trees, of which 902 were used to calculate the PPs. The strains generated in this study were grouped with the ex-type culture *N. rosae* CBS 101057 with support of 0.61/91 with PP and bootstrap (BS), respectively (PP/BS) (Fig. 4). *N. clavispora* was previously reported to cause root and crown rot in Spain and

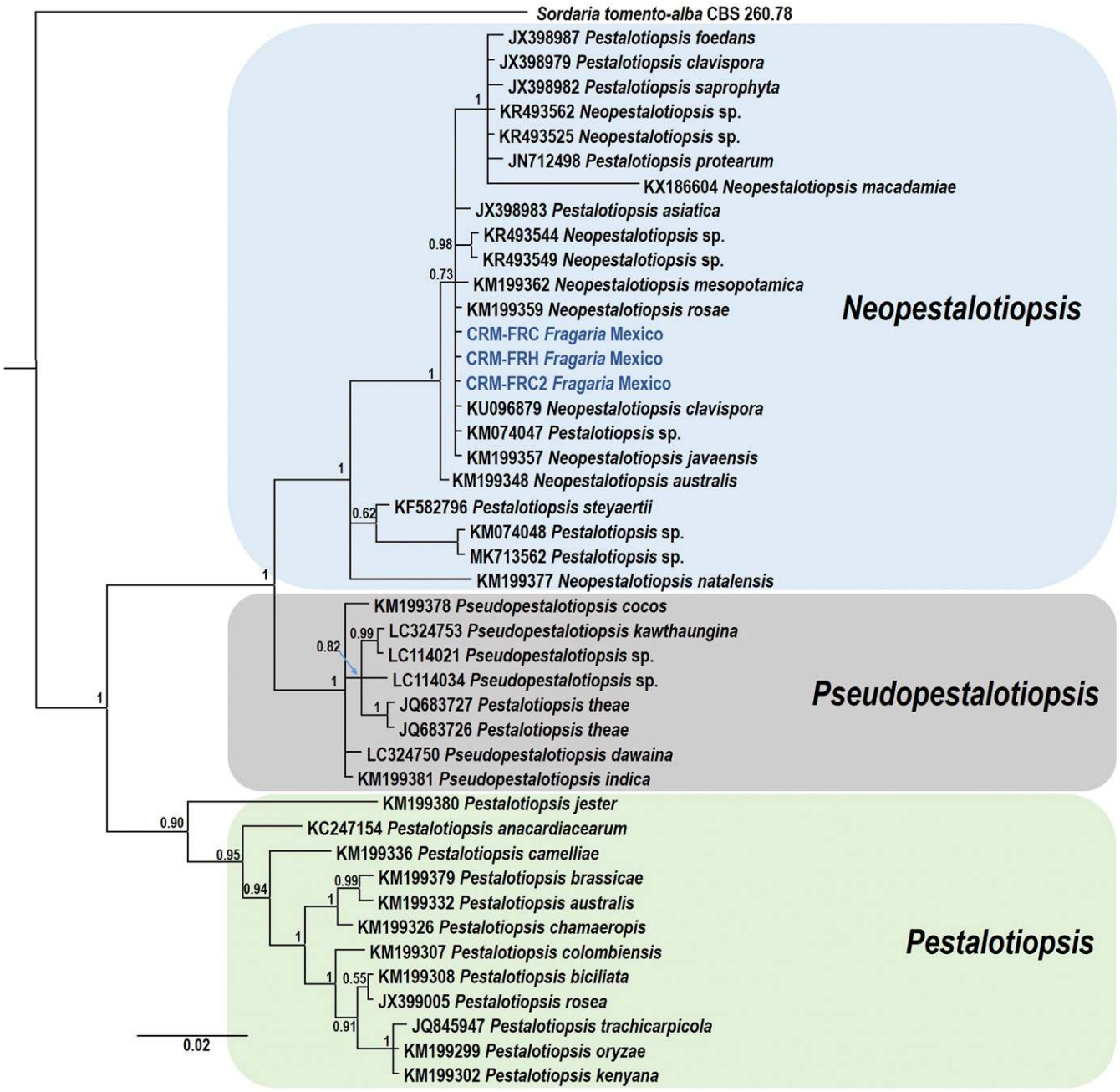

Fig. 3. Bayesian phylogenetic tree reconstructed with species of *Neopestalotiopsis*, *Pseudopestalotiopsis*, and *Pestalotiopsis* genera using the internal transcribed spacer region sequences. Strains in blue (light in print) letters were obtained in this study. Posterior probabilities are indicated in the nodes. *Sordaria tomento-alba* CBS 260.78 sequence was used as outgroup. Scale bar indicates the expected substitutions per site.

was not grouped with the ex-epitype culture but with *N. foedans* with a 0.98/58 support (PP/BS). Therefore, *N. mesopotamica*, *N. iranensis*, and *N. foedans* have been reported from strawberry (Ayoubi and Soleimani 2016; Chamorro et al. 2016), and for the first time in the world, *N. rosae* is also reported from strawberry in this study. In addition, *Pseudopestalotiopsis vietnamensis* was isolated from asymptomatic strawberry leaves in Vietnam with no evidence of pathogenicity (Nozawa et al. 2017).

The pathogenicity tests were conducted with the CRM-FRH and CRM-FRC strains. The inoculum was increased in 250-ml flasks containing rice seeds previously sterilized twice at 15 lb for 18 min and incubated for 2 weeks at 23 ± 2°C. Four-month-old strawberry plug plants of cultivar 'Sayulita' from a commercial nursery (Planasa S.A. de C.V.) were transplanted into 25 × 25-cm plastic bags containing Canadian sphagnum peat moss (Sun Gro Horticulture, Canada). Leaves and crowns were inoculated separately with their corresponding isolates in two different experiments, consisting of groups of 10 plants and the same number for the noninoculated control. In the first experiment, fully expanded leaves were sprayed with 2 ml of 10^6 conidia/ml suspension with 0.05% Tween 20. Inoculated plants were covered with transparent plastic bags for 3 days to favor high relative humidity and kept in greenhouse conditions at 25 ± 2°C. A similar number of plants were inoculated with sterile distilled water as a control. This test was performed twice.

In the second experiment, an equal number of plants were inoculated by making incisions at the base of the crowns with a sterile needle, and then, 10 ml of a 10^6 conidia/ml suspension was added to the crowns (Van Hemelrijck et al. 2017). Another group of 10 plants was used as a control by adding only an equal amount of sterile distilled water. Before inoculation, plants were irrigated to field capacity with tap water.

Leaves of the inoculated plants with the CRM-FRH isolate developed small necrotic spots of approximately 1 to 2 mm 3 days after inoculation. These lesions gradually progressed until they developed into larger spots 10 mm in diameter, frequently in a concentric pattern, 10 days after inoculation. Petiole symptoms first appeared as small black spots that developed 10 days later into sunken black lesions until the leaf wilted because of petiole girdling (Fig. 1). These symptoms were similar to those observed in the field. In crown inoculation, the symptoms showed first as overall stunting and a slight

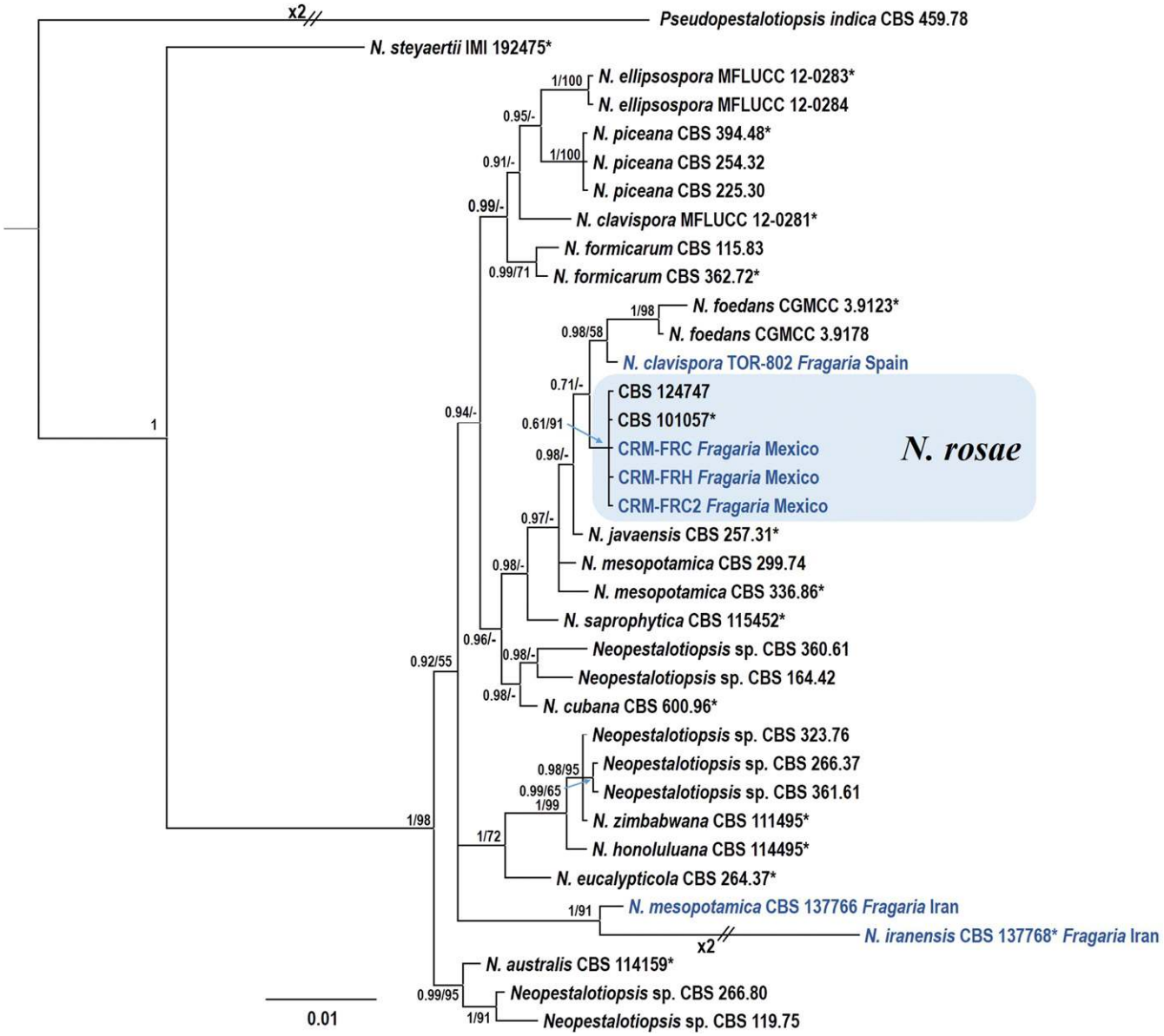

Fig. 4. Bayesian phylogenetic tree of *Neopestalotiopsis* species reconstructed using concatenated datasets of the internal transcribed spacer region, partial β-tubulin, and translation elongation factor 1 α gene sequences. Strains in blue (light in print) letters represent species of *Neopestalotiopsis* reported in *Fragaria* around the world, in which sequences from Mexico obtained in this study belong to *N. rosae*. Sequences of ex-types are indicated with an asterisk. Posterior probabilities and bootstrap support values (PP/BS) are indicated in the nodes. *Pseudopestalotiopsis indica* CBS 459.78 sequence was used as an outgroup. Scale bar indicates the expected substitutions per site.

yellowing of the outer leaves, which soon collapsed. This pattern continued toward the inner leaves, ending in plant collapse 2 to 3 months after inoculation. Part of the roots of diseased plants were brown to black, whereas others remained white. When split open, crowns showed reddish-brown color, intertwined with pearly areas with a dark edge, similar to those observed in the field.

To determine the in vitro effect of commonly used fungicides in strawberries, the CRM-FRH and CRM-FRC isolates of *N. rosae* were used. Commercial formulations and label-recommended field rates of the fungicides azoxystrobin (375 mg/liter) as Amistar (Syngenta, Mexico), fluxapyroxad + pyraclostrobin (312.5 + 312.5 mg/liter) as Merivon (BASF Agro Mexico), boscalid + pyraclostrobin (504 + 256 mg/liter) as Cabrio (BASF Agro), captan (1,250 mg/liter) as Captan 50 (ADAMA, Mexico), iprodione (1,875 mg/liter) as Rovral (FMC Mexico), fludioxonil + cyprodinil (937 + 625 mg/liter) as Switch (Syngenta, S.A. de C.V.), prochloraz (781 mg/liter) as Sportak (FMC, Mexico), and difenoconazole (312.5 mg/liter) as Score (Syngenta Mexico) were used. The rates tested in vitro were determined based on a volume of 400 liters/ha of water application in the field. The corresponding amount of fungicide was diluted in sterile distilled water, added to 9-mm Petri dishes with PDA culture medium previously cooled to 55°C, and then incubated at laboratory conditions (23 ± 2°C). For the quinone outside inhibitor fungicides, 100 mg/liter of salicylhydroxamic acid (Sigma-Aldrich) was added to the growth medium (Wise et al. 2008). Five repetitions (plates) were considered for each fungicide. A completely randomized design was used in this experiment.

After the PDA medium solidified, a 5-mm agar plug was obtained from the marginal area of cultures and placed in the center of the plate and incubated on a laboratory bench at room temperature. The same number of Petri dishes was used as a control without fungicide for each of the products. Seven days later, when the mycelium covered the Petri dishes in the control plates, the radial growth of the fungus was measured in two perpendicular directions, and the average of both measurements was obtained. The experiment was performed twice, and the repetition was considered in the data analysis as a random effect. With the mycelial growth data, an analysis of variance and mean comparison were performed using Proc Glimmix in the SAS system (SAS version 9.4) and a least significant difference mean comparison test ($\alpha = 0.05$). The results indicated that there was a significant interaction between isolates and treatments (isolate × fungicide: $F = 17.99$, $P < 0.001$) in the inhibition of mycelial growth variable. Overall, the leaf isolate tended to grow significantly more in the presence of fungicides containing azoxystrobin and pyraclostrobin than in the presence of the other fungicides compared with the crown rot isolate. The inhibition of mycelial growth (%) in the crown isolate was as follows: azoxystrobin (79.4 ± 0.36), captan (100 ± 0.36), fluxapyroxad + pyraclostrobin (84.85 ± 0.36), pyraclostrobin + boscalid (81.47 ± 0.36), iprodione (100 ± 0.36), difenoconazole (100 ± 0.36), prochloraz (100 ± 0.36), and cyprodinil + fludioxonil (100 ± 0.36). For the leaf isolate, the inhibition of mycelial growth with the same fungicides was as follows: azoxystrobin (85.0 ± 0.36), captan (100 ± 0.36), fluxapyroxad + pyraclostrobin (87.50 ± 0.36), pyraclostrobin + boscalid (85.29 ± 0.36), iprodione (100 ± 0.36), difenoconazole (100 ± 0.36), prochloraz (100 ± 0.36), and cyprodinil + fludioxonil (100 ± 0.36).

In conclusion, the results indicated that the causal agent of the root rot, crown rot, and leaf spot of strawberry transplants in Mexico was *N. rosae*. This investigation is the first report of this pathogen associated with strawberry in Mexico and worldwide. In vitro tests indicated that the pathogen was sensitive to the fungicides captan, fludioxonil + cyprodinil, difenoconazole, and iprodione. Because of the dynamics of plant material importation (mother plants and transplants) every season, there is no information regarding the source of the primary infections. Given the impact of the disease, the results will be used to conduct a more extensive study at the regional level and to take action to contribute to the implementation of an integrated disease management strategy based on the determination of the sources of primary inoculum and the disease epidemiology.

Literature Cited

Ayoubi, N., and Soleimani, M. J. 2016. Strawberry fruit rot caused by *Neopestalotiopsis iranensis* sp. nov., and *N. mesopotamica*. Curr. Microbiol. 72:329-336.

Chamorro, M., Aguado, A., and De los Santos, B. 2016. First report of root and crown rot caused by *Pestalotiopsis clavispora* (*Neopestalotiopsis clavispora*) on strawberry in Spain. Plant Dis. 100:1495.

Darriba, D., Taboada, G. L., Doallo, R., and Posada, D. 2012. jModelTest 2: More models, new heuristics and parallel computing. Nat. Methods 9:772.

Doyle, J. J., and Doyle, J. L. 1990. Isolation of plant DNA from fresh tissue. Focus 12:13-15.

Gilardi, G., Bergeretti, F., Gullino, M. L., and Garibaldi, A. 2019. First report of *Neopestalotiopsis clavispora* causing root and crown rot on strawberry in Italy. Plant Dis. 103:2959.

Glass, N. L., and Donaldson, G. 1995. Development of primer sets designed for use with PCR to amplify conserved genes from filamentous ascomycetes. Appl. Environ. Microbiol. 61:1323-1330.

Hall, T. A. 1999. BioEdit: A user friendly biological sequence alignment editor and analysis program for windows 95/98/NT. Nucleic Acids Symp. Ser. 41: 95-98.

Juárez-Vázquez, S. B., Silva-Rojas, H. V., Rebollar-Alviter, A., Maidana-Ojeda, M., Osnaya-González, M., and Fuentes-Aragón, D. 2019. Phylogenetic and morphological identification of *Colletotrichum godetiae*, a novel pathogen causing anthracnose on loquat fruits (*Eriobotrya japonica*). J. Plant Dis. Prot. 126:593-598.

Machín, A., González, P., Vicente, E., Sánchez, M., Estelda, C., Ghelfi, J., and Silvera-Pérez, E. 2019. First report of root and crown rot caused by *Neopestalotiopsis clavispora* on strawberry in Uruguay. Plant Dis. 103: 2946.

Maharachchikumbura, S. S. N., Hyde, K. D., Groenewald, J. Z., Xu, J., and Crous, P. W. 2014. *Pestalotiopsis* revisited. Stud. Mycol. 79:121-186.

Mertely, J., Chamorro, M., and Peres, N. A. 2015. *Pestalotiopsis* spp., a newly discovered root pathogen of strawberry transplants. Phytopathology 105(Suppl.): S4.95.

Morales-Mora, L. A., Martínez-Salgado, S. J., Valencia de Ita, M. A., Andrade-Hoyos, P., Silva-Rojas, H. V., and Romero-Arenas, O. 2019. First report of leaf spot and anthracnose caused by *Pestalotiopsis* sp. on strawberry in Puebla, Mexico. Plant Dis. 103:2668.

Nozawa, S., Yamaguchi, K., Yen, L. T. H., Hop, D. V., Phay, N., Ando, K., and Watanabe, K. 2017. Identification of two new species and a sexual morph from the genus *Pseudopestalotiopsis*. Mycoscience 58:328-337.

O'Donnell, K., and Cigelnik, E. 1997. Two divergent intragenomic rDNA ITS2 types within a monophyletic lineage of the fungus *Fusarium* nonorthologous. Mol. Phylogenet. Evol. 7:103-116.

O'Donnell, K., Kistler, H. C., Cigelnik, E., and Ploetz, R. C. 1998. Multiple evolutionary origins of the fungus causing Panama disease of banana: Concordant evidence from nuclear and mitochondrial gene genealogies. Proc. Natl. Acad. Sci. U.S.A. 95:2044-2049.

Obregón, V. G., Meneguzzi, N. G., Ibañez, J. M., Lattar, T. E., and Kirschbaum, D. S. 2018. First report of *Neopestalotiopsis clavispora* causing root and crown rot on strawberry plants in Argentina. Plant Dis. 102:1856.

Ronquist, F., Teslenko, M., van der Mark, P., Ayres, D. L., Darling, A., Höhna, S., Larget, B., Liu, L., Suchard, M. A., and Huelsenbeck, J. P. 2012. MrBayes 3.2: Efficient Bayesian phylogenetic inference and model choice across a large model space. Syst. Biol. 61:539-542.

Silvestro, D., and Michalak, I. 2012. raxmlGUI: A graphical front-end for RAxML. Org. Divers. Evol. 12:335-337.

Van Hemelrijck, W., Ceustermans, A., Campenhout, J. V., Lieten, P., and Bylemans, D. 2017. Crown rot in strawberry caused by *Pestalotiopsis*. Acta Hortic. 1156:781-786.

White, T. J., Bruns, T., Lee, S. B., Taylor, J. W., Innis, M. A., Gelfand, D. H., and Sninsky, J. J. 1990. Amplification and direct sequencing of fungal ribosomal RNA genes for phylogenetics. Pages 315-322 in: PCR Protocols: A Guide to Methods and Applications. M. A. Innis, D. H. Gelfand, J. J. Sninsky, and T. J. White, eds. Academic Press, New York, NY.

Wise, K. A., Bradley, C. A., Pasche, J. S., Gudmestad, N. C., Dugan, F. M., and Chen, W. 2008. Baseline sensitivity of *Ascochyta rabiei* to azoxystrobin, pyraclostrobin, and boscalid. Plant Dis. 92:295-300.